# Theory of subsurface occupation, ordered structures, and order-disorder transitions for hydrogen on Pd(111)

Murray S. Daw and Stephen M. Foiles
*Sandia National Laboratories, P.O. Box 969, Livermore, California 94550*
(Received 30 May 1986)

The embedded-atom method (EAM) is applied to the calculation of the structure and phase diagram of H/Pd(111). Many-atom interactions are included inherently in the EAM, leading to substrate-mediated adatom interactions. The EAM predicts the occupation of both surface and subsurface sites forming two $(\sqrt{3}\times\sqrt{3})R\,30°$ structures at coverages of $\Theta=\frac{1}{3}$ and $\frac{2}{3}$ monolayers. Zero-point energy corrections to the classical energies are required. In addition, the EAM is combined with Monte Carlo simulations to predict the critical temperatures of the order-disorder transformation. The symmetries of the predicted structures agree with the experimental low-energy electron diffraction patterns. The predicted critical temperatures of 120 and 110 K at $\Theta=\frac{1}{3}$ and $\frac{2}{3}$ monolayers, respectively, are in excellent agreement with the experimental values of 85 and 105 K.

## I. INTRODUCTION

A recent experiment by Felter *et al.*[1] has discovered two ordered phases for H adsorbed on Pd(111) near 100 K, the lowest critical temperature known for hydrogen on a transition-metal surface. Low-energy electron diffraction (LEED) experiments show the existence of $(\sqrt{3}\times\sqrt{3})R\,30°$ diffraction spots for hydrogen coverages $\Theta$ estimated to be near $\frac{1}{3}$ and $\frac{2}{3}$ monolayers. The intensity of the extra spots as a function of coverage is at a maximum at these two hydrogen coverages and a minimum for intermediate values of the coverage. At the higher-coverage maximum the system disorders at $T_c=105$ K, and at the lower-coverage maximum it disorders at $T_c=85$ K.

The embedded-atom method (EAM) (Refs. 2 and 3) is applied here and also in Ref. 1 to the theoretical investigation of H/Pd(111). The EAM is a semiempirical method of calculating total energies where the empirical parameters are determined by fitting only to *bulk* data. Remarkable agreement was found in that the EAM (without fitting to surface data) predicted not only the correct ordered structures for H/Pd(111) but also the critical temperatures to within better than 50 K.

An important conclusion of our joint theoretical and experimental work[1] was that the hydrogen atoms are adsorbing on surface *and subsurface* threefold sites (see Fig. 1). The surface threefold hollow sites will be denoted in this paper as the *surface tetrahedral* and *surface octahedral* sites. The two subsurface sites are located in the "subsurface plane" which is *between the first and second atomic planes of the Pd lattice,* and will be denoted as the *subsurface octahedral* and *subsurface tetrahedral* sites. The term "subsurface" is here reserved for sites between the top two metal planes. The distinction between tetrahedral and octahedral for surface sites is based on the symmetry the site would have if the metal lattice were continued. The surface octahedral sites are thus the threefold hollow sites which have a Pd atom directly below them in the second metal layer and the surface tetrahedral site have a Pd atom directly below them in the third metal layer. The subsurface tetrahedral sites are threefold sites which have a Pd atom directly below in the second metal layer and the subsurface octahedral sites are threefold sites with a Pd atom directly below in the third metal layer. Note that the surface tetrahedral site is located directly above the subsurface octahedral site, and the sur-

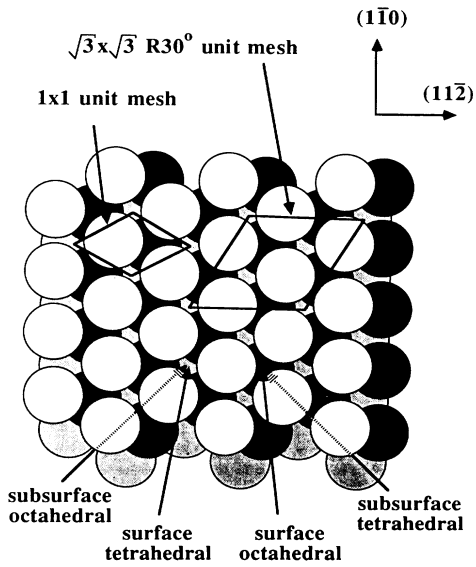


FIG. 1. Structure of the Pd(111) surface with the top three metal layers shown (first layer is white, second layer is darkly shaded, and third layer is lightly shaded). The $1\times1$ unit cell is shown, along with the $(\sqrt{3}\times\sqrt{3})R\,30°$ unit cell obtained after hydrogen exposure. Four possible hydrogen adsorption sites are indicated, all of threefold symmetry: surface tetrahedral, surface octahedral, subsurface tetrahedral, and subsurface octahedral. The surface sites are above the first metal plane, while the subsurface sites are between the first and second metal planes. The subsurface tetrahedral site is rarely occupied, due to energetics.

 

face octahedral site is directly above the subsurface tetrahedral site. In Ref. 1, we calculated that the subsurface octahedral sites are very close in energy to the surface adsorption sites. We predicted that at very low temperatures the ordered structures are hexagonal arrays consisting entirely of hydrogen occupying *subsurface octahedral sites*. The energetics are illustrated in Fig. 2, which shows that the subsurface octahedral site is in fact very close to the surface tetrahedral site in energy. Figure 2 is presented as a schematic illustration because the actual energy minima and barriers are very sensitive to the overall coverage and to the local distribution of hydrogen atoms.

It is interesting to contrast these results for Pd to those for H/Ni(111), which exhibits one ordered $2\times2$ pattern[4] at $\Theta=\frac{1}{2}$ with $T_c=250$ K. The surface structure proposed for H/Ni(111) places the hydrogen atoms in the surface threefold hollow sites in an open hexagonal array. (The inequivalent threefold hollow sites were assumed to be degenerate.)

Another theoretical approach to the H/Pd(111) system has been taken by Muscat[5] as part of a systematic study of hydrogen on several close-packed transition metal surfaces. The calculations, based on the embedded cluster method, indicate that the multiple-adatom interactions can be described very accurately by pair interactions. Excellent agreement with experiment is obtained for the case of H/Ni(111). However, for H/Pd(111) the predicted ordered structures is $2\times2$, in clear contradiction to the experimentally observed $(\sqrt{3}\times\sqrt{3})R\,30°$ structure. Furthermore, the subsurface sites were investigated and found to be energetically unfavorable in the embedded-cluster method.

The results of the embedded-atom method in Ref. 1 by contrast not only found that the subsurface sites were very close in energy to the surface adsorption site, but that the inclusion of these sites in the calculation of the ordered structures was essential in obtaining agreement with the experiment.

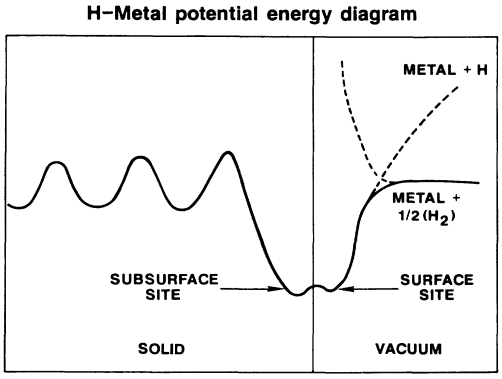


FIG. 2. Schematic potential-energy diagram for a hydrogen atom interacting with Pd(111). The figure illustrates the energetics calculated using the embedded-atom method, which are strongly dependent on coverage. The spatial coordinate is along a path which passes through the surface tetrahedral and subsurface octahedral sites (see Fig. 1). Note that in addition to the minimum at the usual "surface" site, the energy has a minimum also at a subsurface site, below the top Pd layer. The sites further into the bulk than the subsurface site are bulklike. (From Ref. 1.)

The possibility of subsurface sites for H on Pd surfaces has been suggested by several workers. Behm *et al.*[6] have reviewed the experimental evidence. In particular, they find a low-temperature peak in the thermal desorption spectra of Pd(110), which they associate with hydrogen in a "subsurface" state. However, unlike the (111) surface, the (110) surface of Pd undergoes a $(1\times2)$ reconstruction at coverages above one monolayer and the "subsurface" site for that case may be associated with that reconstruction. Similar thermal desorption spectra are obtained for H/Ni(110) at high coverages.[7] Psueodpotential calculations[8] have investigated the possibility that certain photoemission features observed for H/Pd(111) might be explained by the occupation of subsurface sites (in particular, the subsurface octahedral sites). The calculations suggest that the disappearance of H-induced features in the photoemission spectra is consistent with hydrogen occupying subsurface octahedral sites, but the results are inconclusive.

Nørskov[9] performed total-energy calculations for H/Ni(111) using the effective-medium theory, a method with some similarities to that used here, except that metal atom relaxations were not included. Nørskov concluded that it is unlikely that the subsurface octahedral site on Ni(111) is competitive with the surface threefold sites as an absorption site. Similar results have been obtained by the present authors, using the methods detailed here, for the case of H/Ni(111).

In this paper, the details of the calculations summarized in Ref. 1, for H/Pd(111) are presented. The calculations use the recently developed embedded-atom method.[2,3] The results show that the adsorption sites are the surface threefold hollow sites and the subsurface octahedral sites located between the first two metal planes. The preferred ordered structures and corresponding critical temperatures are also determined over the coverage range $0\leq\Theta\leq1$, by coupling the EAM to Monte Carlo techniques. The results are in excellent agreement with the independently determined experimental phase diagram.

## II. THEORY

In the embedded-atom method (EAM),[2,3] the total energy of a system of atoms is given by

$$E_{\rm tot}=\sum_i F_i(\rho_{h,i})+\tfrac{1}{2}\sum_{i,j,j\neq i}\phi_{ij}(R_{ij})\ . \tag{1}$$

In the first summation, $\rho_{h,i}$ is the background electron density at atom $i$ due to the rest of the atoms in the system thought of as the host, and $F_i$ is the embedding energy of placing an atom into that electron density. In the second summation, $\phi_{ij}$ is a short-range interaction representing electrostatic repulsion. The expression for the total energy [Eq. (1)] can be obtained from density functional theory by viewing each atom as being embedded in a sea of electrons created by all the other atoms. Assuming that this host electron density contributed by the surrounding atoms is suitably uniform at each atom,

the embedding energy is then a function of the electron density at the site. In this framework the embedding energy provides most of the cohesive energy of the solid, viewed as a binding between the atom and the host electron density. There is an embedding function for each element in the system (in the present case $F_{\mathrm{Pd}}$ and $F_{\mathrm{H}}$) which is assumed to be universal in that the function depends only on the type of atom and the electron density but is independent of the other atomic types present in system. The electrostatic repulsions are short-ranged and relatively weak.

The expression in Eq. (1) is useful provided one has a description of the host electron density for each atom (i.e., electron density established by all the other atoms). In this work, we approximate the electron density in the solid by a superposition of atomic electron densities:

$$\rho_{h,i}=\sum_{j\neq i}\rho_j^a(R_{ij})\ . \tag{2}$$

In this case, the total energy is a simple function of the positions of the atoms.

For any assemblage of H and Pd atoms, we then require the following functions to calculate the total energy: $F_{\mathrm{Pd}}(\rho)$, $F_{\mathrm{H}}(\rho)$, $\rho^a_{\mathrm{Pd}}(r)$, $\rho^a_{\mathrm{H}}(r)$, $\phi_{\mathrm{Pd\text{-}Pd}}(r)$, $\phi_{\mathrm{Pd\text{-}H}}(r)$, and $\phi_{\mathrm{H\text{-}H}}(r)$. These functions have been obtained semiempirically by Daw and Baskes.[2,3] The functions are determined by fitting to bulk properties of Pd: lattice constant, elastic constants, vacancy formation energy, sublimation energy, difference in energy between fcc and bcc phases, and the H heat of solution. The complete set of functions has been described in detail by Daw and Baskes,[3] and we have used those functions unchanged for the present work. It is to be emphasized that the functions were fitted to *bulk* properties. There has been no fitting to the surface properties.

It is important to note that the EAM [Eqs. (1) and (2)] gives a framework for treating both adsorbate and substrate atoms uniformly. As such, the EAM is in contrast to the related effective-medium[9,10] and quasiatom[11] techniques. The latter techniques have concentrated on the calculation of heats of adsorption and solution, while not being concerned with the metal atom relaxations. The EAM, because it includes the metal atom energetics, allows calculations of both adsorbate and substrate relaxations, *as well as adsorbate-adsorbate interactions mediated by the substrate.* The computational simplicity of the method allows the treatment of the large unit cells needed to study disordered systems. Thus, both ordered and random states of the system can be treated on the same footing.

The EAM has been applied successfully to the study of many other transition metal and alloy properties, including the structure of liquid metals,[12] bulk phonons,[13] basic alloy properties,[14] alloy surface segregation,[15] unreconstructed, clean metal surfaces,[3,14] and the reconstruction of Pt(110).[16] The method has been shown in these previous publications to give a reasonable description of bulk and surface properties.

Three types of calculations using the EAM will be considered here: energy minimization, zero-point energy analysis, and Monte Carlo simulations. In all cases, the calculations are performed for a (111) slab geometry with periodic boundary conditions in the plane of the slab along the $[1\,\bar{1}\,0]$ and $[1\,1\,\bar{2}]$ directions. Hydrogen atoms are placed on one face of the slab. It is found that using slabs that are four atomic planes thick yields results for the hydrogen energies in agreement to better than 0.02% (0.0005 eV/H) with results for much thicker slabs.

The energy minimization calculations find the local classical-energy minimum. These calculations allow for the displacement of all atoms in the system, i.e., both Pd and H. These calculations use a slab with a $6\times6$ surface unit mesh. The minimization is performed by a conjugate gradient algorithm.[17]

As will be discussed in the results section, the zero-point energy contributions are important for determining the lowest energy structures. A complete determination of the quantum motion of a single chemisorbed hydrogen atom on Ni surfaces has been undertaken with a related method, the effective-medium theory.[18] For the present work, we will compute the zero-point energies *at coverage* by performing a harmonic mode analysis[13] of the slab about the classical-energy minimum. The zero-temperature energy of a given ordered structure is then taken to be the sum of the classical-energy minimum plus the zero-point energy.

The Monte Carlo calculations are performed using the usual Metropolis[19] algorithm by moving one atom at a time. These calculations use a slab with a $9\times6$ surface unit mesh (the first direction being along $[1\,\bar{1}\,0]$). Three types of displacements were included in the simulations: small displacement of a hydrogen atom from its current position, small displacement of a top layer Pd atom from its current position, and jumps of hydrogen atoms to an unoccupied, nearby adsorption site. In this way the simulations incorporated both the spatial relaxation of both the metal and hydrogen atoms as well as the change in site occupancy of the hydrogen. The details of the simulations will be discussed in the results section.

Molecular dynamics calculations of the atomic motion are also feasible using the EAM. For the Pd(111) surface, however, the slow hopping times for the hydrogen at the temperatures of interest ($\sim$100 K) requires impractically long computer runs for the determination of reliable statistical averages.

## III. RESULTS

We describe in the following the calculations for H/Pd(111) using the embedded-atom method. Much of the theoretical work on surface phase transitions uses pair- or trio-interaction models of the energetics.[20] While we will estimate the size of the pair interactions, we emphasize that the calculations presented in this paper are *not* done using a two-body approximation, but rather with the full, many-atom EAM formulation. That the higher-body interactions are important will be discussed in detail in what follows.

### A. Clean surface

The top-layer spacing of the clean Pd(111) surface is calculated to contract slightly by 0.07 Å. While we know

of no measurements of this spacing on Pd(111), results on Ni(111) indicate a small contraction[21] of $0.025 \pm 0.025$ Å. The surface energy is computed to be 1070 ergs/cm$^2$. Again, we do not know of a measurement of this value. The average surface energy has been estimated from liquid surface tension data[22] to be 2000 ergs/cm$^2$ and from the heat of sublimation[23] to be 1600 ergs/cm$^2$. Given the uncertainty of these estimates and the fact that the (111) surface is the lowest energy face, the calculated value is not unreasonable. We have found no tendency toward reconstruction of this surface, in agreement with experiment.[1]

### B. Low hydrogen coverage

The energy of a single hydrogen atom on Pd was calculated by placing a hydrogen atom in an ideal site in the metal slab and then allowing for all local distortions to find the minimum energy. The harmonic zero-point energy is then added in to obtain the total energy. The candidate sites included octahedral and tetrahedral sites (on the surface these are the two, inequivalent threefold hollow sites), the twofold bridge on the surface, the on-top site on the surface, and several saddle-point positions between the various local minimum sites. We find only the following sites to be favorable: the subsurface octahedral and tetrahedral sites, and the surface octahedral and tetrahedral sites (see Table I). The subsurface octahedral site is slightly lower in energy than the two surface sites, and the subsurface tetrahedral site is the highest in energy. We find the surface and subsurface sites to be distinctly lower in energy than the bulk octahedral sites. We also find the sites between the second and third layer of metal atoms to be essentially bulklike. The surface twofold bridge site was found to be a saddle point about 0.2 eV higher in energy than the surface threefold hollows. The on-top site is about 0.5 eV higher in energy than the surface threefold hollows. The on-top site is about 0.5 eV higher in energy than the surface threefold hollows.

Table I summarizes the adsorption energies of these different surface-related sites for the low coverage limit as well as the classical and zero-point energy contributions. (The energies are relative to the free atom.) The calculated energies of the bulk interstitial sites are given for comparison. There are several points to notice about these results. First, the energies of all four sites are within 0.02 eV, suggesting that there would be some occupation of all types of sites at room temperature. Second, the two surface sites are degenerate. Third, the zero-point energies are significant. The subsurface tetrahedral site has the lowest classical energy, yet the zero-point energy resulting from the smaller size of this site causes it to be the least favorable of the four sites. Fourth, the adsorption energies computed here are in reasonable accord with the experimental value[24] of 2.85 eV. The reader should keep in mind that results discussed in the next section show that *the size of the energy difference for occupying surface and subsurface sites changes at higher coverages.*

We have schematically summarized the calculated energetics of hydrogen on Pd(111) in Fig. 2. The figure is schematic because the details of the energetics depend sensitively on coverage. Note that the subsurface octahedral site is comparable in energy to the surface tetrahedral site, and that the barrier between these two sites is relatively small. Note also that sites deeper into the bulk are bulklike.

The relaxation of the metal atoms is moderately important for the results presented in Table I. The calculations of Table I allowed for all relaxations of the metal atoms. If, on the other hand, the calculations are done by first minimizing the clean surface, then freezing the substrate and adding hydrogen, the relative ordering of the sites remains the same as in Table I, but the absolute energies shift. The subsurface tetrahedral site has a large relaxation energy of 0.36 eV, while the other three sites are on the order of a few hundredths of an eV. The metal atom relaxation is significant only for metal atoms immediately adjacent to the hydrogen. For a clean surface, as we have noted, the top metal interlayer spacing is reduced from the bulk-terminated value. As hydrogen is added, however, the top-layer metal atoms neighboring a surface or subsurface hydrogen atom move outward, expanding the first metal interlayer spacing locally. This spacing expands back to nearly the bulk-terminated value. This expansion in the top metal interlayer spacing is essentially complete by a coverage of $\Theta = \frac{1}{3}$.

The classical diffusion barriers between these sites at low coverages have also been determined. Metal atom relaxations are, of course, very important for these calculations, and have been included here. For diffusion in either the surface or subsurface plane, the barriers are about 0.2 eV while the barrier between surface and subsurface planes is only 0.05 eV. It is important to note that these barrier heights increase significantly with the addition of

TABLE I. Calculated single hydrogen adsorption energies *at low coverage* (in eV, relative to an isolated hydrogen atom) for different adsorption sites on Pd(111) and the calculated energies of the bulk interstitial sites for comparison. The total energy is in the sum of classical-energy minimum and harmonic zero-point energy. The adsorption sites are defined in the text and in Fig. 1.

| Site | $E_{\text{classical}}$ | $E_{\text{zero-point}}$ | $E_{\text{tot}}$ |
|---|---|---|---|
| Surface tetrahedral | −2.926 | 0.271 | −2.655 |
| Surface octahedral | −2.926 | 0.271 | −2.655 |
| Subsurface tetrahedral | −2.950 | 0.318 | −2.632 |
| Subsurface octahedral | −2.905 | 0.249 | −2.660 |
| Bulk tetrahedral | −2.483 | 0.302 | −2.181 |
| Bulk octahedral | −2.536 | 0.031 | −2.505 |
| (third-layer interstitial sites are essentially bulklike) | | | |

more hydrogen and represent only the *classical* diffusion barrier.

In the next section, we will calculate the energies of ordered structures at higher coverages. Nevertheless, some qualitative understanding can be gained by studying the H-H interactions at low coverage. Because the EAM inherently includes many-atom interactions, the difference between the predictions of the pair-interaction model and the full EAM give insight into the importance of many-body interactions. In fact, we find that the assumption of pair additivity of the energy is quantitatively poor.[25] We have estimated the pair interactions from the energy of two hydrogen atoms on the surface relative to the adsorption energies of single atoms in the two sites. In general, the interactions are repulsive. Recall from Fig. 1, that the surface tetrahedral and subsurface octahedral sites are on top of each other (when viewed along the [1 1 1] direction); we will call the combination of surface tetrahedral and subsurface octahedral sites a "type-$A$ vertex." The same arrangement is true for the surface octahedral and subsurface tetrahedral sites, and these we call a "type-$B$ vertex." The repulsive pair interaction between hydrogen atoms in the surface and subsurface positions of the same vertex is about 0.2 eV. Note that on the (111) surface, a vertex of one type is surrounded by three, nearest-neighbor vertices of the opposite type. The repulsive interaction between hydrogen atoms on nearest-neighbor vertices is also around 0.2 eV except for the interaction between the surface octahedral site and its neighboring subsurface octahedral site which is 0.14 eV. The repulsive interaction between hydrogen atoms on second and third neighbor vertices ranges from 0.07 to 0.11 eV and the interaction at greater distances is very small. The important observation is that two hydrogen atoms will avoid occupying the same or nearest-neighbor vertices. Also, the interactions between hydrogen atoms occupying second- and third-neighbor vertices are comparable to each other and weaker than for first neighbors. These interactions are different from the ones calculated using embedded-cluster techniques for H/Pd(111) by Muscat.[5] Muscat's results involve only surface-surface interactions, and show that the nearest-neighbor interaction is strongly repulsive, the second neighbor is about 0.01 eV, the third neighbor is less than 0.001 eV in magnitude, and the sixth neighbor is $-0.01$ eV. The interactions described by Muscat lead to the prediction of an ordered $2\times2$ pattern for H on Pd(111), in clear contradiction to the experimental observations of Felter *et al.*[1]

The source of the H-H interaction in the framework of the EAM is easily understood. For simplicity, consider the interaction of hydrogen atoms occupying only the surface sites. On the clean surface, each Pd atom has an embedding energy of $F_{\rm Pd}(\rho_S)$, where $\rho_S$ is the electron density at a surface Pd atom. An adsorbed H atom contributes a density $\rho_{\rm H}$ to three surface Pd neighbors, each of which now has an embedding energy of $F_{\rm Pd}(\rho_S+\rho_{\rm H})$. Nearest-neighbor hydrogen atoms share two substrate Pd atoms, each of which has an embedding energy of $F_{\rm Pd}(\rho_S+\rho_{\rm H}^{(1)}+\rho_{\rm H}^{(2)})$ where the superscripts denote the two different hydrogen atoms. Expanding this last embedding energy in a Taylor series, assuming the $\rho_{\rm H}$'s to be small compared to $\rho_S$, and subtracting out the single-atom adsorption energies, gives a nearest-neighbor interaction energy of $2F''_{\rm Pd}(\rho_S)\rho_{\rm H}^{(1)}\rho_{\rm H}^{(2)}$ where the factor of 2 comes from the number of substrate atoms that have two H nearest neighbors. Because $F''_{\rm Pd}(\rho_S)>0$, and $\rho_{\rm H}>0$, this interaction is repulsive. Repeating the argument for second-nearest-neighbor hydrogen atoms gives an interaction of $F''_{\rm Pd}(\rho_S)\rho_{\rm H}^{(1)}\rho_{\rm H}^{(2)}$ because in this case only one substrate atom has two H neighbors. This argument roughly accounts for the ratio of first- to second-nearest-neighbor interaction. Further since second- and third-nearest neighbors share the same number of Pd atoms, their pair energies should be similar, as is seen. Thus, the EAM naturally leads to the prediction of a substrate-mediated H-H interaction. The nature of this interaction is different from that investigated by other workers.[5,26–28] In the EAM, the significant H-H interactions are short-ranged, being most significant when two hydrogen atoms neighbor the same substrate atom.

Of further interest, is the observation that the H-H interaction depends on $F''_{\rm Pd}(\rho_S)$. This quantity is affected by the top metal interlayer spacing and hence on the overall coverage. Therefore, we expect a dependence of the effective two-body interaction on the overall coverage, especially for $\theta<\frac{1}{3}$. This coverage-dependence is generally neglected in most lattice-gas models.[5,20]

It is very important to note that many-H interactions are not negligible; strict use of the preceding H-H pair energies at finite coverages can lead to 30% errors compared to using the complete energy calculation. The EAM inherently accounts for many-H interactions. This implies, however, that H-H pair-interaction models of the ordered phases of H neglect important effects, and that even including trio interactions may be insufficient for a complete description.[25]

### C. Ordered structures

The excess energy per surface metal atom (energy relative to the linear interpolation in hydrogen coverage between the clean surface and a full monolayer) has been computed for the ideal ordered structures with the following symmetries:

$$1\times1,\ (\sqrt{3}\times\sqrt{3})R\,30^\circ\ \ (\theta=1)\,,$$

$$(\sqrt{3}\times\sqrt{3})R\,30^\circ,\ (\sqrt{12}\times\sqrt{12})R\,30^\circ\ \ (\theta=\tfrac{1}{3},\tfrac{2}{3})\,,$$

$$2\times1,\ 2\times2\ \ (\theta=\tfrac{1}{2})\,.$$

The energy considered is the sum of the classical-energy minimum and harmonic zero-point correction. For each of these symmetries, the different assignments of the atoms to the various surface and subsurface sites consistent with that symmetry were considered. Figure 3 plots the results for the lowest energy structure found for each symmetry. For the $\sqrt{3}$ structures at $\theta=\frac{1}{3}$ and $\frac{2}{3}$ monolayers, the lowest energy structures occupied only the subsurface octahedral sites. (For simplicity, the abbreviations $\sqrt{3}$ and $\sqrt{12}$ will be used to refer to the above symmetries.) In the lowest energy $\sqrt{12}$ structure at $\Theta=\frac{1}{3}$, the unit cell contained two subsurface octahedral

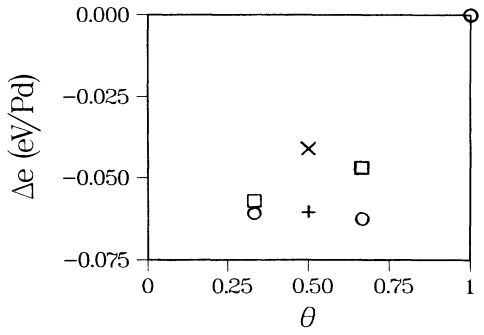


FIG. 3. Calculated excess energies of ordered hydrogen superstructures on Pd(111). (Excess energy is the difference between the energy and a linear function connecting the low-coverage and monolayer limits.) The symbols represent the following symmetries: ○, $(\sqrt{3}\times\sqrt{3})R°$; □, $(\sqrt{12}\times\sqrt{12})R\,30°$; +, $2\times1$; ×, $2\times2$. Harmonic zero-point energies and optimal site occupations have been included. (From Ref. 1.)

hydrogen atoms and two subsurface tetrahedral hydrogen atoms while at $\Theta=\frac{2}{3}$ the unit cell is composed of four subsurface octahedral hydrogen atoms and four surface octahedral hydrogen atoms. The lowest $\sqrt{12}$ structure is higher in energy than the lowest $\sqrt{3}$ structure. For the half-monolayer structures, the lowest energy $2\times1$ case has all the hydrogen in the subsurface octahedral site and the lowest energy $2\times2$ has half in the subsurface octahedral and half in the surface octahedral. At full monolayer coverage, the lowest-energy structure with $1\times1$ symmetry (not shown in the Fig. 3) has all the hydrogen atoms in the subsurface octahedral site but the energy is lower for the $\sqrt{3}$ structure where a third of the hydrogen atoms are moved to the surface tetrahedral site.

The energy per hydrogen atom is a monotonically increasing function of coverage. Examining the lowest energy structures, which have $\sqrt{3}$ symmetry, we find the following values for the energy per hydrogen atom (this is not the same as the chemical potential, which is related to the derivative of the energy with respect to coverage). At the low coverage extreme, the adsorption is into the subsurface octahedral site with an energy per hydrogen atom of $-2.660$ eV/H (from Table I). At $\Theta=\frac{1}{3}$, the adsorption is into the subsurface octahedral site with an energy per hydrogen atom of $-2.648$ eV/H. At $\theta=\frac{2}{3}$, all of the hydrogen is in subsurface octahedral sites, with an energy per hydrogen atom of $-2.558$ eV/H. At $\Theta=1$, the surface tetrahedral site is occupied in addition to subsurface octahedral sites, and the energy per hydrogen atom jumps to $-2.479$ eV/H. These results are consistent with the saturation of the chemisorption[1] above $\Theta=\frac{2}{3}$, as well as the coverage dependence of the chemisorption energy reported by Engel and Kuipers.[29]

The energy differences between the various arrangements of the atoms in the unit cell are fairly small. For the $\sqrt{3}$ structure at $\Theta=\frac{1}{3}$, the next best structure places all the atoms in the surface tetrahedral site with an energy difference of 0.023 eV per hydrogen atom relative to the optimal arrangement. At $\Theta=\frac{2}{3}$, the next best $\sqrt{3}$ structure alternates the hydrogen atoms between the subsurface octahedral site and the surface tetrahedral site. The energy for this structure is 0.006 eV per hydrogen atom higher than the optimal structure.

The role of the subsurface octahedral site in determining the ordered structure can be demonstrated by considering the ordered states containing hydrogen in the two surface sites only. In that case the $(\sqrt{12}\times\sqrt{12})R\,30°$ structures are very nearly degenerate with the $(\sqrt{3}\times\sqrt{3})R\,30°$ structures. In fact there are several possible ordered structures with various symmetries that have nearly the same energy. These alternate ordered structures are created by shifting rows of hydrogen atoms. The hydrogen atoms in the alternate structures have a similar environment to the $\sqrt{3}$ structures except that some second neighbors have been converted to third neighbors. In addition, these alternate structures occupy both the surface octahedral and surface tetrahedral sites. These structures are nearly degenerate because the effective second- and third-neighbor interactions are very similar and the two inequivalent surface sites are degenerate. The presence of these numerous, nearly degenerate ordered states makes ordering unlikely, in disagreement with experimental observation. In the next section, we will show that Monte Carlo simulations allowing only surface site occupation verify these conclusions. Therefore, we conclude that *the occupation of subsurface sites is necessary for the theory to agree with experiment.*

The equilibrium position of the hydrogen in the subsurface octahedral site also changes with coverage. At zero coverage, the hydrogen sits 0.7 Å below the top Pd layer while at higher coverages the Pd-H bond length increases as its equilibrium position moves towards the geometrical center of the octahedral site which is 1.1 Å below the top Pd layer. (Similar effects are true for the H in a surface site.)

The increase in bond length with coordination is a common chemical effect. A simple argument shows that it occurs naturally in the EAM. The equilibrium condition for atom $i$ is, from Eqs. (1) and (2):

$$F_i'(\rho_{h,i})\sum_{j\neq i}(\rho_j^a)'(R_{ij})+\sum_{j\neq i}F_j'(\rho_{h,j})(\rho_i^a)'(R_{ij})+\sum_{j\neq i}\phi_{ij}'(R_{ij})=0\ . \quad (3)$$

With increasing coordination, $\rho_{h,j}$ increases. Because $F'<0$ and $F''>0$, $F'$ will decrease in magnitude with increasing $\rho_{h,j}$. To maintain equilibrium, the spacings must increase in order to reduce the values of $\phi$ (a positive, monotonically decreasing function). Thus the presence of the high coverage of hydrogen would be expected to increase both the metal interlayer spacing as well as the metal-hydrogen distances in accord with the detailed calculations.

In order to determine the zero-temperature phase equilibria, it is important to consider the energy of structures off ideal stoichiometry. Away from the ideal coverages of $\frac{1}{3}$, $\frac{2}{3}$, and 1 monolayers, the lowest energy distribution of hydrogen atoms considered still had $\sqrt{3}$ symmetry. The excess energy of the lowest energy $\sqrt{3}$ structures as a function of composition is plotted in Fig. 4. For

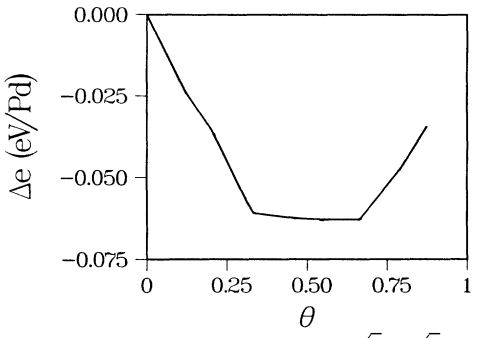


FIG. 4. Calculated excess energies of $(\sqrt{3}\times\sqrt{3})R30°$ structures off of ideal coverages. See the text for an explanation of the unit cell. (From Ref. 1.)

$\Theta<\frac{1}{3}$, the lowest energy structures correspond to occupying one subsurface octahedral site in each $\sqrt{3}$ unit cell with a fractional probability. For $\frac{1}{3}<\theta<\frac{2}{3}$, the lowest energy structures correspond to occupying one subsurface octahedral site in each $\sqrt{3}$ unit cell with unit probability and a second subsurface octahedral site with a fractional probability. Notice that this prescription gives a lower energy $\sqrt{3}$ structure at $\Theta=\frac{1}{2}$ than the $2\times1$ or $2\times2$ structures. For $\Theta>\frac{2}{3}$, two subsurface octahedral sites are occupied with unit probability and a surface tetrahedral site is occupied with fractional probability. The most important feature of these results is that the energy versus coverage is concave upwards in the region between $\Theta=\frac{1}{3}$ and $\frac{2}{3}$ monolayers. This implies that at zero temperature for coverages between $\frac{1}{3}$ and $\frac{2}{3}$ there is no phase separation into regions of $\frac{1}{3}$ and $\frac{2}{3}$ coverages. Rather, a uniform phase of intermediate coverage is formed.

### D. Phase diagram

In order to determine the finite-temperature phase diagram, Monte Carlo simulations were performed for coverages between $\frac{1}{3}$ and $\frac{2}{3}$. The simulations proceeded by jumping (changing the position of) one atom at a time using the usual Metropolis algorithm.[19] Namely, a jump is always accepted if it lowers the energy and for jumps producing an energy increase of $\Delta E$, the jump is accepted with a probability of $\exp(-\Delta E/k_bT)$. This procedure produces an ensemble of atomic configurations appropriate to the temperature $T$. The properties of the system are then measured by averaging over these configurations. Three types of atomic displacements were incorporated into the simulations. First, metal atoms in the top layer were allowed to make small displacements from their current position. The remaining metal atoms of the system were held fixed to reduce the computer time. Zero-temperature calculations at a variety of coverages showed no evidence of significant relaxation of second-layer metal atoms, so it was assumed that the motion of the top-layer atoms was sufficient to allow for the changes in the local geometry of the surface and subsurface H adsorption sites. Second, the hydrogen atoms were allowed to make small displacements about their current location. This is important because, as discussed above, the equilibrium position of the hydrogen atom changes with the local environment. Thus it is essential that the hydrogen atoms can relax their positions in accord with changes in their local environment. Finally, the hydrogen atoms could be moved from one adsorption site to any other unoccupied adsorption site on the surface. These sites included surface and subsurface octahedral and tetrahedral sites. The inclusion of jumps between sites is necessary to attain the equilibrium distribution of hydrogen atoms between sites in a reasonable length of computer time. The distribution of the atoms between adsorption sites was not treated in a simple lattice-gas framework because, as discussed in the preceding section, the interaction energies between the hydrogen atoms depend on the local environment in part through the changes in the equilibrium positions of the hydrogen and surface Pd atoms.

The current simulations used a rectangular periodic cell with nine unit lengths in the $[1\,\bar{1}\,0]$ direction and six in the $[1\,1\,\bar{2}]$ direction. This cell has 192 adsorption sites (48 of each of the four types). A coverage of $\Theta=\frac{1}{3}$ involves 16 hydrogen atoms distributed among the available sites. The shape and size of this unit cell is compatible with $(\sqrt{3}\times\sqrt{3})R30°$, $(\sqrt{12}\times\sqrt{12})R30°$, $2\times1$, and $2\times2$ symmetries. (Only ordered structures corresponding to the $\sqrt{3}$ symmetry were ever observed to form, as is consistent with the energetics discussed in the preceding section.) It should be noted that the size of the simulation cell is small enough that there could be significant finite-size shifts in the critical temperatures determined from the simulations. However, such shifts should not affect the general features of the phase diagram determined below.

The energy differences used in the simulations were computed using the *full EAM energy* expression corrected for zero-point energy. It is not feasible to compute the change in zero-point energy completely for each atomic jump considered. Thus a simplified treatment of the zero-point energy was used for the Monte Carlo simulations: namely, each hydrogen atom was assumed to possess a zero-point energy that depended only on the type of site it occupied (i.e., independent of neighboring H or local Pd relaxations). The values of these site-dependent zero-point energies were taken from the zero-coverage calculations performed above. This prescription should be reasonable as long as there is little coupling between the vibrational modes of the nearby hydrogen atoms. Zero-point energy calculations of ordered structures at higher coverages suggest that this approximation is good at $\Theta=\frac{1}{3}$ but can lead to errors of a few hundredths of an eV per hydrogen at higher coverages. The comparison also suggests that at higher coverages the use of the low-coverage zero-point energy underestimates the preference for occupation of the subsurface octahedral site.

When using simulation techniques to study order-disorder phenomena, it is important to insure that the results are not an artifact of the initial conditions. The simulations were therefore performed in two sets. First, simulations were made starting with an initially random arrangement of hydrogen atoms. In some cases, order annealed in during the course of the simulation. The highest temperature at which annealing occurred determined a lower bound for the critical temperature. The second set

started with an ordered structure. In those cases where disorder resulted, an upper bound on the critical temperature is obtained. The combination of information from two different starting conditions ensures that disordered states do not simply represent simulations too short to produce order. Note that the simulations were not performed at ideal coverages. For example, near $\Theta=\frac{2}{3}$, the simulations were performed by removing one of the 32 hydrogen atoms from the periodic cell producing a coverage of $\Theta=\frac{31}{48}$ rather than $\frac{32}{48}$. This greatly reduced the computer time needed for equilibration because the presence of vacancies or extra atoms provides a lower energy path between the ordered and disordered states.

Two pieces of information about the distribution of the hydrogen atoms were obtained from the simulations. The first is the two-dimensional geometric structure factor of the hydrogen, $S$. This is defined by

$$S(\mathbf{k})=\left|\sum_n \exp(i\mathbf{k}\cdot\mathbf{X}_n)\right|^2, \tag{4}$$

where $\mathbf{k}$ is a two-dimensional wave vector and $\mathbf{X}_n$ is the position of atom $n$ in the plane of the surface. $S(\mathbf{k})$ is proportional to the kinematic approximation to the scattering intensity from the hydrogen if one assumes that the scattering factors of the hydrogen at the same for all four adsorption sites. In this context, it simply provides a quantitative measure of the presence of order. In addition to the structure factor, the mean number of hydrogen atoms in each of the different types of adsorption sites was determined.

The simulation results for $\Theta=0.64$ are summarized in Figs. 5 and 6. Figure 5 shows the value of the structure factor, evaluated at $\mathbf{k}$ corresponding to the $\sqrt{3}$ symmetry, as a function of temperature. Note that it decreases

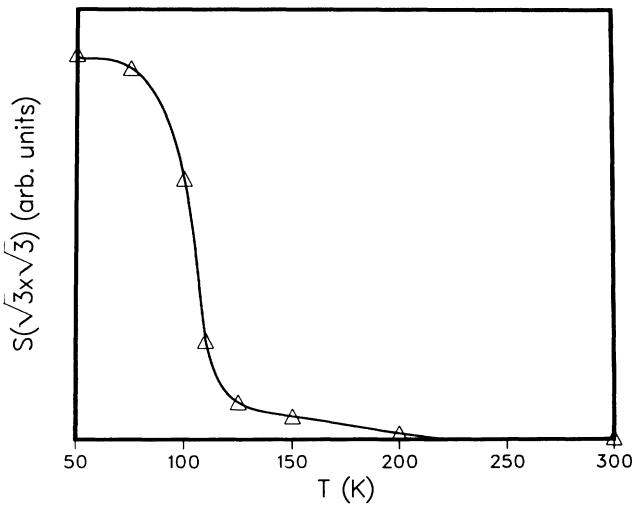


FIG. 5. Calculated geometric structure factor corresponding to the $(\sqrt{3}\times\sqrt{3})R30°$ LEED spot as a function of temperature for $\Theta=0.64$. The open triangles are results from the simulations, and the solid line is drawn as a guide to the eye. The critical temperature is inferred from the inflection point in the curve.

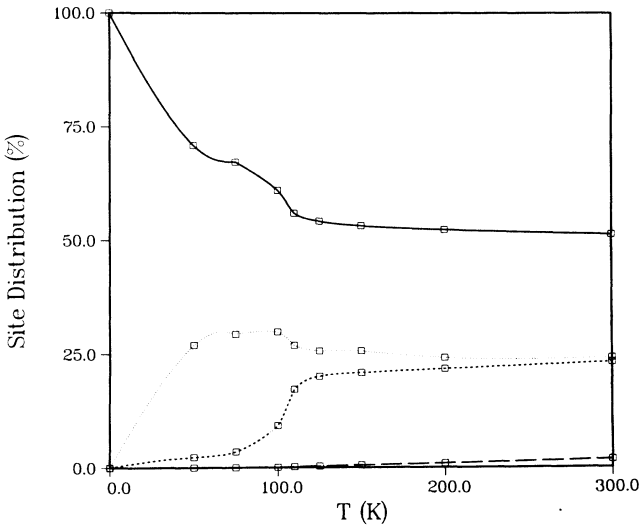


FIG. 6. Calculated site distribution for H as a function of temperature for $\Theta=0.64$. The open squares represent results of the simulations and the lines are drawn as guides. The solid line is for subsurface octahedral, the dotted line for surface tetrahedral, the dashed line for surface octahedral, and the dot-dashed line for subsurface tetrahedral. The critical temperature at this coverage is calculated to be at 110 K.

sharply around 110 K which therefore corresponds to the critical temperature at this coverage. Figure 6 shows the distribution of the hydrogen atoms between the different adsorption sites as a function of temperature. The simulations performed for $\Theta=0.69$ show very similar behavior except that the critical temperature is somewhat lower, about 95 K. Note that below the critical temperature, the hydrogen mostly occupy the subsurface octahedral sites with the rest of the hydrogen atoms in the surface tetrahedral sites located directly above the sites that would be occupied in the ideal ordered structure. This represents the fact that the lowest energy excitation of the ordered system is to move an atom from a subsurface octahedral site to the surface site directly above it. Above the critical temperature, about half of the hydrogen atoms are in the subsurface octahedral site with the rest divided between the two inequivalent surface sites. There is never much occupation of the subsurface tetrahedral site.

The simulations performed for $\Theta=0.31$, show a critical temperature of around 120 K. Three more series of simulations were performed at $\Theta=0.46$, 0.56, and 0.97. All of these coverages have much lower critical temperatures, near or below 50 K. This information enables us to predict the approximate phase diagram shown in Fig. 7. Note that Fig. 7 also contains the experimental results for this system. The agreement between theory and experiment is extremely encouraging, especially considering that no adjustment to surface properties has been made. It should be noted that the approximation used for the zero-point energy should cause the critical temperatures to be underestimated at higher coverages.

The effects of the occupation of subsurface sites on the phase diagram can be seen by performing the Monte Carlo simulations allowing only surface-site occupation. In

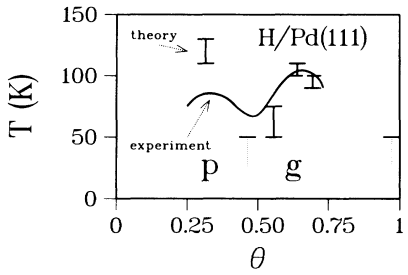


FIG. 7. Calculated and experimental phase diagrams for H/Pd(111). The "$p$" denotes the "primitive" $(\sqrt{3}\times\sqrt{3})R\,30°$-1H structure (i.e., $\Theta=\frac{1}{3}$), and the "$g$" denotes the "graphite-like" $(\sqrt{3}\times\sqrt{3})R\,30°$-2H structure (i.e., $\Theta=\frac{2}{3}$). The experimental results are from Ref. 1.

this case, $(\sqrt{3}\times\sqrt{3})R\,30°$ structures which deviate very slightly from the ideal stoichiometries of $\Theta=\frac{1}{3}$ and $\frac{2}{3}$ monolayers are found to disorder at very low temperatures. In fact, it is found that *random* structures formed from surface sites alone can have energies within less than 0.001 eV/H of the energy of the *ordered* structures formed from surface sites alone. Thus ordered structures would not be formed for temperatures above a few degrees. Only at precisely ideal stoichiometry can an ordered structure appear to remain ordered in the Monte Carlo simulations. Clearly, these results are in contradiction with experiment. When the subsurface sites are included in the simulations, this situation is resolved and the phase diagram of Fig. 7 is obtained. Thus the experimental observation of ordering provides evidence for the significant occupation of subsurface sites on this surface.

## IV. CONCLUSIONS

The embedded-atom method has been applied to a calculation of the ordered phases of H on Pd(111). The EAM is semiempirical, relying on known properties of the *bulk* H-Pd system. The calculations indicate that hydrogen-hydrogen interactions are mediated by the substrate and that the many-body contributions to the energy are crucial to the determination of the critical temperature. Occupation of the subsurface octahedral site is predicted in addition to the occupation of surface threefold sites. Based on the calculated critical temperatures, we have determined the phase diagram for H/Pd(111) and compared it to experiment. The agreement with experiment is remarkably good.

## ACKNOWLEDGMENTS

The authors would like to thank Dr. T. E. Felter, Dr. R. H. Stulen, Dr. C. F. Melius, and Mr. C. L. Bisson of this laboratory, and Professor L. D. Roelofs of Haverford College for very useful discussions. This work was supported by the U.S. Department of Energy (Office of Basic Energy Sciences).

[1]T. E. Felter, S. M. Foiles, M. S. Daw, and R. H. Stulen, Surf. Sci. Lett. **171**, L379 (1986).
[2]Murray S. Daw and M. I. Baskes, Phys. Rev. Lett. **50**, 1285 (1983).
[3]Murray S. Daw and M. I. Baskes, Phys. Rev. B **29**, 6443 (1984).
[4]K. Christmann, R. J. Behm, G. Ertl, M. A. Van Hove, and W. H. Weinberg, J. Chem. Phys. **70**, 4168 (1979).
[5]J.-P. Muscat, Phys. Rev. B **33**, 8136 (1986).
[6]R. J. Behm, V. Penka, M. G. Cattania, K. Christmann, and G. Ertl, J. Chem. Phys. **78**, 7486 (1983).
[7]K. Christmann, F. Chehab, V. Penka, and G. Ertl, Surf. Sci. **152**, 356 (1985).
[8]C. T. Chan and S. G. Louie, Phys. Rev. B **30**, 4153 (1984), and references therein.
[9]J. K. Nørskov, Phys. Rev. Lett. **22**, 1734 (1980).
[10]J. K. Nørskov, Phys. Rev. B **26**, 2875 (1982).
[11]M. J. Stott and E. Zaremba, Phys. Rev. B **22**, 1564 (1980).
[12]S. M. Foiles, Phys. Rev. B **32**, 3409 (1985).
[13]M. S. Daw and R. D. Hatcher, Solid State Commun. **56**, 697 (1985).
[14]S. M. Foiles, M. I. Baskes, and M. S. Daw, Phys. Rev. B **33**, 7983 (1986).
[15]S. M. Foiles, Phys. Rev. B **32**, 7685 (1985).
[16]M. S. Daw, Surf. Sci. Lett. **166**, L161 (1986).
[17]J. E. Sinclair and R. Fletcher, J. Phys. C **7**, 864 (1972).
[18]M. J. Puska, R. M. Nieminen, M. Manninen, B. Chakraborty, S. Holloway, and J. K. Nørskov, Phys. Rev. Lett. **51**, 1081 (1983).
[19]N. Metropolis, A. W. Rosenbluth, M. N. Rosenbluth, A. H. Teller, and E. Teller, J. Chem. Phys. **21**, 1087 (1953).
[20]L. D. Roelofs, T. L. Einstein, N. C. Bartelt, and J. D. Shore, Surf. Sci. **176**, 295 (1986).
[21]J. E. Demuth, P. M. Marcus, and D. W. Jepsen, Phys. Rev. B **11**, 1460 (1975).
[22]W. R. Tyson and W. A. Miller, Surf. Sci. **62**, 267 (1977).
[23]W. R. Tyson, Can. Metall. Q. **14**, 307 (1975).
[24]H. Conrad, G. Ertl, and E. E. Latta, Surf. Sci. **4**, 435 (1974).
[25]L. D. Roelofs, S. M. Foiles, and M. S. Daw (unpublished).
[26]T. L. Einstein and J. R. Schrieffer, Phys. Rev. B **7**, 3629 (1983).
[27]A. G. Eguiluz, D. A. Campbell, A. A. Maradudin, and R. F. Wallis, Phys. Rev. B **30**, 5449 (1984).
[28]P. Nordlander and S. Holmstrom, Surf. Sci. **159**, 443 (1985).
[29]T. Engel and H. Kuipers, Surf. Sci. **90**, 1623 (1979).

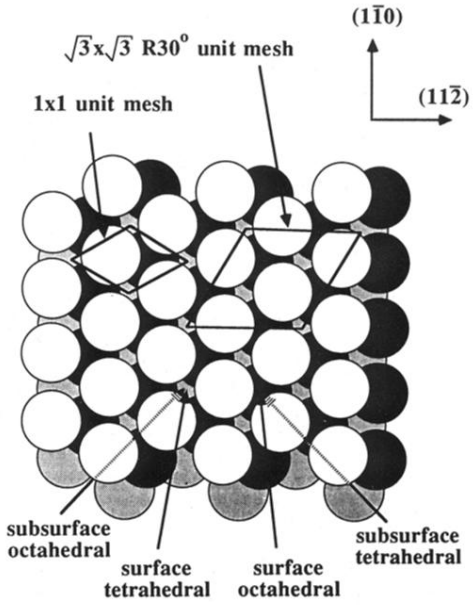


FIG. 1. Structure of the Pd(111) surface with the top three metal layers shown (first layer is white, second layer is darkly shaded, and third layer is lightly shaded). The $1\times1$ unit cell is shown, along with the $(\sqrt{3}\times\sqrt{3})R\,30°$ unit cell obtained after hydrogen exposure. Four possible hydrogen adsorption sites are indicated, all of threefold symmetry: surface tetrahedral, surface octahedral, subsurface tetrahedral, and subsurface octahedral. The surface sites are above the first metal plane, while the subsurface sites are between the first and second metal planes. The subsurface tetrahedral site is rarely occupied, due to energetics.